

# Noise-like pulse based on four-wave-mixing with photonic crystal fiber filled by reduced graphene oxide

Lei Gao, Tao Zhu,\* Wei Huang, and Min Liu

Key Laboratory of Optoelectronic Technology & Systems (Ministry of Education), Chongqing University, Chongqing 400044, China

\*Corresponding author: [zhutao@cqu.edu.cn](mailto:zhutao@cqu.edu.cn)

A noise-like pulse based on four-wave-mixing (FWM) in a fiber cavity with photonic crystal fiber filled by reduced graphene oxide is proposed. Due to large evanescent field provided by 3 cm photonic crystal fiber and ultrahigh nonlinearity of reduced graphene oxide, this mixed structure provides excellent saturable absorption and high nonlinearity, which are necessary for generating FWM. We experimentally prove that the laser transfers its energy from center wavelength to sidebands through degenerate FWM due to modulation instability, and new subsidebands are generated via cascaded FWM among those sidebands. The frequency spacings of the sidebands are far larger than the longitudinal mode spacing, and various orders of longitudinal modes of the fiber cavity are supported by the cascaded FWM. As the new frequencies are generated not simultaneously, their phases are loosely fixed, resulting in low coherent noise-like pulse rather than fully coherent pulse train. © 2014 Optical Society of America

OCIS Codes: (060.3510) Lasers, fiber, (060.4370) Nonlinear optics, fibers, (190.4380) Nonlinear optics, four-wave mixing

Passively mode-locked fiber laser (ML) has drawn intense interests in both science and industry, and the engineering with dispersion, loss and gain, filtering, polarization, and nonlinearity makes it functioning in various states, such as conventional soliton, self-similar laser, dissipative soliton, etc [1-3]. Particularly, when the laser operating condition is altered, or more nonlinear processes are involved, a laser cavity can generate a kind of noise-like pulse (NLP) comprising a bunch of pulses with noise-likely varying width and intensity [4-8]. Compared with soliton lasers, NLP possesses a much lower coherence, and its autocorrelation trace contains a coherence peak of femtosecond duration locating on a broad pedestal ranging from several to hundreds of picoseconds [7]. Its optical bandwidth is often comparable to or even larger than the gain bandwidth of active fiber, and its power can be much larger than that of conventional soliton [6-9]. It has been shown that NLP performs better in generating smooth supercontinuum, as no spectral modulation ever shown around the pump wavelength due to its stochastic character [10], and it can also be used for optical coherence tomography, radar, and sensing requiring low coherence [11].

NLP can be found in laser cavity with net normal or anomalous dispersion, and its formation involves specific nonlinearity, birefringence, gain, and polarization state. The generation of NLP may attribute to cavity nonlinear transmission and walk-off between two polarizations [4], and NLP formed in nonlinear polarization rotation cavity is originated from the combined effect of soliton collapse and positive cavity feedback [12]. Also, the oversaturation of saturable absorber (SA) and excessive nonlinear phase shift may attribute to formation of NLP [13], and Raman self-frequency shift, Raman gain enhancement, and four-wave-mixing (FWM) may increase the spectral width of NLP through zero dispersion fiber or long length of highly nonlinear fiber [6,14].

Here, we propose a NLP based on FWM in a fiber cavity. Conventionally, FWM has been found in fiber cavity with a high fineness Fabry-Perot interferometer or

high Q microresonator, through which light is confined to small volume, and cascaded FWM take place due to enhanced peak power [15,16]. As the free spectral range (FSR) and fineness of Fabry-Perot interferometer are relative high, their adjacent modes, corresponding to different orders of longitudinal modes of the whole laser cavity, can be fully filled with the newly generated frequencies via cascaded FWM. Therefore, stable and coherent soliton train can be generated due to the well fixed frequency spacing of those modes. Specifically, Herr et al have shown that depending on the orders of appearance of the subsidebands, two different FWM processes may exist in a microresonator, and two kinds of pulse with high and low coherence can be formed [16,17]. The physics of the low coherent pulse lies in the fact that the spacing between the pump laser and sidebands that generated originally from the parametric gain is far larger than the FSR of microresonator, and new subsidebands are generated by cascaded FWM among those sidebands. When the pump power is relatively high, the subsidebands merge into a gap-free spectrum. However, as the phases of those subsidebands are slightly different, the formed temporal pulses possess low coherence.

We find that when the frequency spacing between the main wavelength and sidebands that formed due to modulation instability is larger than the fundamental frequency of a fiber cavity, cascaded FWM may occur among the main wavelength and the sidebands. Similar to the FWM process in a microresonator, the loosely fixed phase relation among various orders of longitudinal modes lead to the formation of NLP. The principle of NLP based on cascaded FWM is schematically shown in Fig. 1 (a). Similar to a microresonator with high Kerr coefficient, in a ML ring cavity with high nonlinearity, the laser is destabilized via modulation instability, and the energy of its center wavelength is transferred to sidebands [18]. The frequency spacing between the center wavelength and sidebands is determined by the period of dispersion, nonlinearity, peak power, polarization state, and average net dispersion [18,19]. Comparatively, the frequency

spacing in conventional single fiber (hundreds of GHz) is much larger than the fundamental frequency of a typical fiber cavity (MHz~kHz). Previously, we have observed sidebands with a spacing of 3 nm based on modulation stability in a fiber cavity [18]. Technically, the modulation instability is a degenerate FWM process, where two photons with frequency of  $\omega_0$  are annihilated, and two new photons with Stokes frequency ( $\omega_{mS}$ ) and anti-Stokes frequency ( $\omega_{mAS}$ ) are generated simultaneously. Both the energy conservation ( $2\hbar\omega_0 = \hbar\omega_{mS} + \hbar\omega_{mAS}$ , where  $\hbar$  is the reduced Planck constant,  $m = \pm 1, \pm 2, \dots$ ) and the phase matching condition are satisfied.

When the nonlinearity of a ML cavity is sufficient high, for example, via interacting with material possessing ultrahigh nonlinearity or confining strongly light to vary small area, cascaded FWM may occur in two possible ways: process 1 of FWM involving interaction between sidebands with center wavelength (such as  $\hbar\omega_{1S} + \hbar\omega_{2AS} = \hbar\omega_0 + \hbar\omega_{1AS}$ ), and process 2 of FWM involving multiple mixing among subsidebands without center wavelength. Besides, degenerate FWM may occur in those frequencies. Through cascaded FWM, the energy of center wavelength dissipates into the newly generated frequencies to a large span [17,20]. When pump power is high enough, various orders of the longitudinal modes near main wavelength are supported and phased locked by the cascaded FWM. However, as those modes are generated at different FWM processes, their loosely fixed phase relationship results in randomly variations of width and intensity. This leads to the formation of NLP.

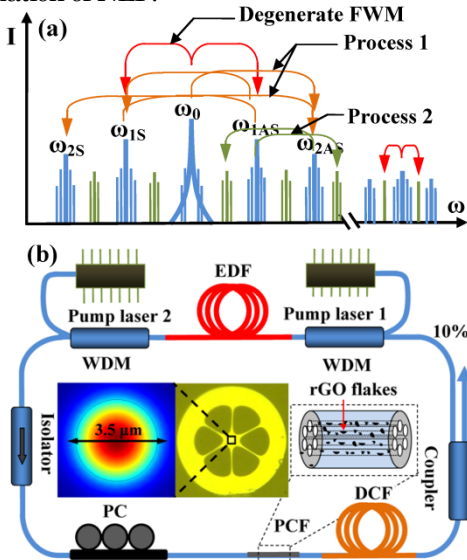


Fig.1 (a), Schematic of cascaded FWM in ML. (b), Schematic setup of the fiber laser cavity.

In this Letter, we experimentally demonstrate the NLP operation based on FWM in a fiber ring cavity with photonic crystal fiber (PCF) filled by reduced graphene oxide (rGO). As a two-dimensional layer of carbon atoms, graphene exhibits excellent saturable absorption due to the Pauli blocking effect, as well as ultrahigh nonlinearity from  $\pi$ -electron conjugation. [21,22]. Experiments have shown that the nonlinearity of graphene membrane can be as high as  $10^{-6}$  esu, and it can be further enhanced by long and intense evanescent field interaction, such as fiber

taper and PCF [23-26]. FWM based on graphene interacting with fiber taper or photonic crystal nanostructure has been reported, where the effective nonlinearity can be enhanced to 1000 times of that without graphene [27-30]. As a special kind of graphene, rGO that synthesized by oxidation of graphite, has been found possessing outstanding SA properties and high nonlinearity [31,32]. We have observed the modulation stability based on 8 mm fiber taper deposited with rGO [18]. However, a longer fiber taper is hard to make, and it is fragile and suffered from environmental contamination. While, filling holes of PCF with rGO provides another solution [25,31]. We enhance the cavity nonlinearity via filling 3 cm PCF with rGO flakes, and NLP is obtained due to FWM.

The setup of fiber cavity is shown in Fig. 1 (b), incorporating 1 m erbium-doped fiber (EDF, Liekki ER 80-8/125) that bidirectionally pumped by two 980 nm lasers through two wavelength division multiplexers (WDMs), a polarization independent isolator, a polarization controller (PC), an optical coupler with 10% output, 19.5 m dispersion compensation fiber (DCF) with dispersion parameter of -38 ps/nm/km, and 8.6 m standard single mode fiber (SMF, Corning SMF-28) with dispersion parameter of 18 ps/nm/km. The net normal dispersion is 0.737 ps<sup>2</sup>. The SA is produced by filling rGO dissolved in N,N-dimethylformamide into the holes of PCF, and dry in 38°C for 24 hours. The parameters of rGO we used and the detail method to make transparent rGO solution is represented in [32], and its size is estimated to be  $\sim 1$   $\mu$ m. The cross section of PCF and its stimulated electric norm distributions of LP<sub>01</sub> mode are shown in Fig. 1 (b). The effective field diameter of 3.5  $\mu$ m guarantees both large evanescent field and relative small insertion loss when deposited by rGO flakes. After evaporation, the PCF is spliced to SMFs, and no interference effect is introduced. The splice loss between pure PCF and SMF is about 3 dB, and the deposition loss of rGO in 3 cm PCF is about 1 dB. The modulation depth of the SA is about 9% detected by a 790 nm laser with duration of 120 fs. The output is monitored by a detector with 2 GHz bandwidth, an oscilloscope (Lecroy, SDA 8600A), a frequency analyzer (Agilent, PSA E4447A), an autocorrelator (APE, Pulse check), and an optical spectrum analyzer (OSA, Yokogawa, AQ6370).

Setting two pump lasers to 200 mW, we rotate PC carefully, and stable NLP can be observed easily. As shown in Fig. 2 (a), the period of pulse train is 145.6 ns, corresponding to a fundamental frequency of 6.874 MHz, and the intensity fluctuation of the train is about 5%. Its autocorrelation trace in Fig. 2 (b) exhibits a pedestal with a full width at half maximum (FWHM) of 730.693 ps, and the coherent spike is about 530 fs. As the pedestal width is comparable to the range of the autocorrelator, a small part of the trace cannot be shown, which has no effect on the discussion here. The FWHM of the optical spectrum in Fig. 2 (c) is 6.3 nm, which is smaller than that in [4-7]. The possible reason is that the FWM is relative weak due to the large insertion loss originating from the splice between PCF with SMFs. The corresponding radio frequency (RF) spectrum in Fig. 2 (d) reveals a contrast ratio of 60 dB near the fundamental frequency, which is

slightly broadened due to the intensity fluctuation. The inset containing RF spectrum to 500 MHz suggests that this NLP has very good stability.

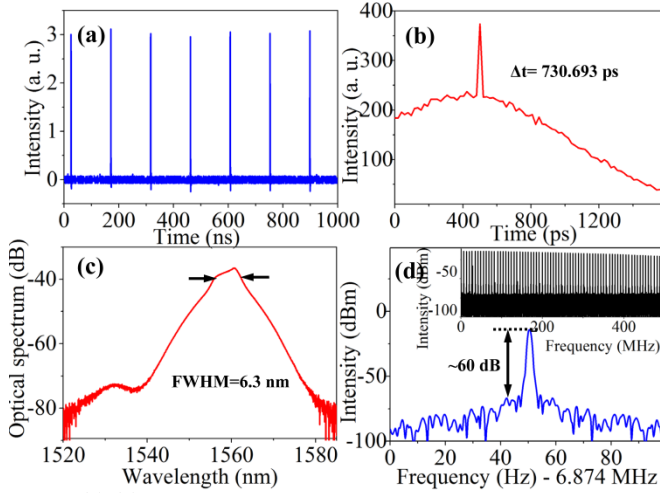


Fig. 2. (a)-(d) Pulse train, autocorrelation trace, optical spectrum, and corresponding RF spectra of NLP.

We examine the effects of SA and DCF in forming NLP. When the DCF is removed from the cavity, no NLP but only conventional soliton can be found, no matter how the PC is adjusted. No NLP could be found when the SA is replaced by that produced by depositing a graphene film produced from chemical vapor deposition between two fiber pigtailed as in [21,22]. Once the SA is removed, neither NLP nor conventional soliton could be found. Those experiments indicate that the rGO-PCF and DCF are key in generating cascaded FWM.

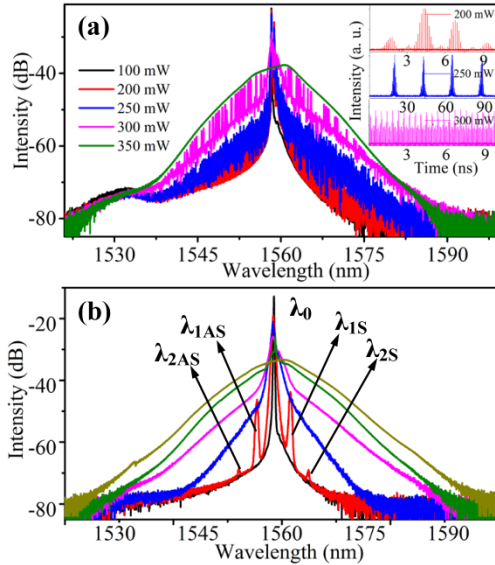


Fig. 3. (a), Optical spectra for different powers of pump 1 with pump 2 as 200 mW, and the insets correspond to temporal trains. (b), Optical spectra under different PC settings with both pump lasers as 200 mW.

The laser states under different pump power are depicted in Fig. 3 (a). The optical spectra are recorded by the OSA with high sensitive mode. It is clearly shown that higher cavity power brings more intense FWM, as its optical spectrum is broadened. The corresponding temporal trains in the insets indicate that a more stable and

regular pulse train is formed when increasing pump power, from randomly pulse (200 mW) to Q-switched mode-locking (250 mW) and unstable mode-locking (300 mW), suggesting that the NLP is generated through FWM.

The optical spectra under different polarization states in Fig. 3 (b) reveals that the laser is destabilized by FWM at first, and then more longitudinal modes are activated through cascaded FWM, finally leads to NLP. During the experiment, we adjusting the PC slowly, making sure that the polarizations state varies gradually. The narrowest spectrum shown in Fig. 3 (b) corresponds to a weakly mode-locked laser, which is destabilized when four new frequencies are generated due to degenerate FWM. This is consistent to our previous observation based on fiber taper deposited with rGO, which is more detail in [18]. Here, we find that the four new wavelengths, namely,  $\lambda_{2AS}=1552.11$  nm,  $\lambda_{1AS}=1555.43$  nm,  $\lambda_0=1558.43$  nm,  $\lambda_{1S}=1561.59$  nm,  $\lambda_{2AS}=1565.03$  nm, both satisfy the energy conservation of the process 1 of FWM, supporting our explanation about the formation process of NLP. As the phase matching condition is optimized, frequencies far from center wavelength broaden gradually when changing PC position. The pulse that mode-locked originally by rGO is destabilized, and the energy is transferred from center wavelength to new sidebands. When the power of center wavelength is comparable to those of the sidebands, NLP is formed.

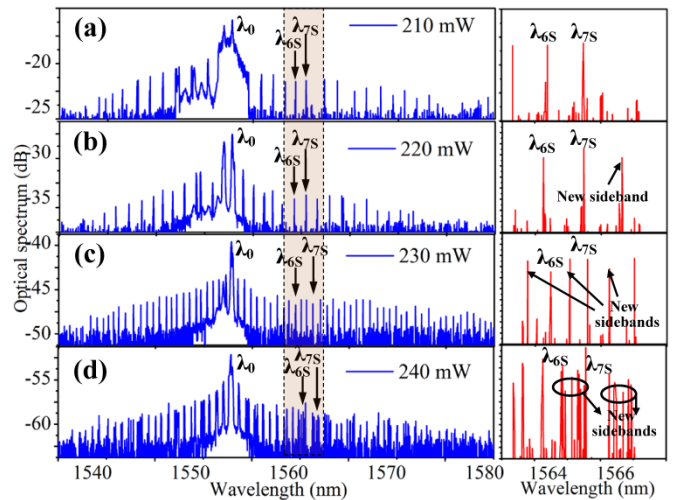


Fig. 4. Optical spectra for different powers of pump 1, and the right figures correspond to the dotted regions in the left.

We record the optical spectra for pump power between 210 mW and 240 mW by the OSA with fast speed mode, which captures data without averaging. Although the temporal output is unstable in this region as in Fig. 3 (a), once the pump power is fixed, the optical spectrum almost keeps constant. We plot part of the optical spectrum between 1563.3 nm and 1567.3 nm on the right side of the figure, and define the subsidebands as  $\lambda_{6S}$  and  $\lambda_{7S}$  according to their position with respect to the main wavelength. As shown in Fig. 4 (a), subsidebands with a spacing of 1.08 nm are generated around the center wavelength for pump power at 210 mW. Clearly, new subsidebands appear in the middle of  $\lambda_{6S}$  and  $\lambda_{7S}$  when the pump power is increased to 230 mW, and more dense

frequencies are generated for pump power at 240 mW. Meanwhile, the spacing increases to 1.22 nm for pump power at 220 mW, then decreases to 1.12 nm for pump power at 230 mW. The increase of the spacing is due to the increment of the pump power, while its decrease is caused by the decreased peak power when part of cavity energy is transferred to new subsidebands. As the lasing process is so fast, we cannot record the generation process of the sidebands with a spacing of 3.16 nm as in Fig. 3 (b). However it is reasonable to attribute the generation of subsidebands with spacing of  $\sim 1.2$  nm to the FWM among the sidebands with spacing of  $\sim 3.16$  nm initialized by modulation instability. We note that the spacing of  $\lambda_{6S}$  and  $\lambda_{7S}$  ( $\sim 1.2$  nm) is less than half of the spacing of  $\lambda_{1S}$  and  $\lambda_{2S}$  (1.58 nm) as in Fig. 3 (b), and this is because the pump powers and polarization states are different in the two cases. Hence, the energy of center wavelength is transferred into subsidebands with more intense cascaded FWM, which is consistent to the results in Fig. 3.

Considering the results shown in Figs. 3 and 4, we can reasonably conclude the formation process of NLP based on cascaded FWM. When pump power is increased, the laser transfers its energy from center wavelength to sidebands through degenerate FWM due to modulation instability. New subsidebands can be generated via cascaded FWM among those sidebands. When the pump power is high enough, the newly generated frequencies merge into a gap-free spectrum, and various orders of longitudinal modes of the fiber cavity are supported. As those modes are generated in different FWM processes, their phases are loosely fixed, and it results in the formation of NLP rather than a fully coherent pulse train.

In summary, we proposed a NLP in a fiber cavity with PCF filled by rGO based on cascaded FWM. Experiment demonstrates that energy of the center wavelength of the laser is transferred to sidebands through degenerate FWM, and new frequencies are generated via cascaded FWM among those sidebands. As the frequencies are not generated simultaneously, the phases of longitudinal modes of this fiber ring cavity are loosely fixed, resulting to NLP with noisily varying of duration and width. Our works provide new information in understanding the dynamics of ML with high nonlinearity, and also find a new way to generate NLP, which may find applications in smooth supercontinuum generation, optical coherence tomography, and sensing.

This work was supported by National Natural Science Foundation of China (No. 61405020, 61475029 and 61377066) and the Outstanding Youth Science Fund Project of Chongqing.

## References

1. M. E. Fermann, and I. Hartl, *Nature Photon.* **7**, 868 (2013).
2. X. Liu, D. Han, Z. Sun, C. Zeng, H. Lu, D. Mao, Y. Cui, F. Wang, *Sci. Rep.* **3**, 2718 (2013).
3. K. Kieu, W. H. Renninger, A. Chong, and F. W. Wise, *Opt. Lett.* **34**, 593 (2009).
4. M. Horowitz, Y. Barad, and Y. Silberberg, *Opt. Lett.* **22**, 799 (1997).
5. L. M. Zhao, D. Y. Tang, J. Wu, X. Q. Fu, and S. C. Wen, *Opt. Express* **15**, 2145 (2007).
6. L. M. Zhao, D. Y. Tang, T. H. Cheng, H. Y. Tam, and C. Lu, *Opt. Commun.* **281**, 157 (2008).
7. Y. Jeong, L. Zuniga, S. Lee, and Y. Kwon, *Opt. Fiber Technol.* **20**, 575 (2014).
8. A. Runge, C. Aguergaray, N. Broderick, and M. Erkintalo, *Opt. Lett.* **38**, 4327 (2013).
9. T. North, and M. Rochette, *Opt. Lett.* **38**, 890 (2013).
10. S. Lin, S. Hwang, and J. Liu, *Opt. Express* **22**, 4152 (2014).
11. S. Keren, and M. Horowitz, *Opt. Lett.* **26**, 328 (2001).
12. D. Y. Tang, L. M. Zhao, and B. Zhao, *Opt. Express* **13**, 2289 (2005).
13. Q. Wang, T. Chen, M. Li, B. Zhang, Y. Lu, and K. P. Chen, *Appl. Phys. Lett.* **103**, 011103 (2013).
14. L. A. Vazquez-Zuniga, Y. Jeong, *Photon. Technol. Lett.* **24**, 1549 (2012).
15. J. Schröder, T. D. Vo, and B. J. Eggleton, *Opt. Lett.* **34**, 3902 (2009).
16. T. Herr, K. Hartinger, J. Riemensberger, C. Y. Wang, E. Gavartin, R. Holzwarth, *Nature Photon.* **6**, 480 (2012).
17. F. Ferdous, H. Miao, D. E. Leaird, K. Srinivasan, J. Wang, L. Chen, L. T. Varghese, and A. M. Weiner, *Nature Photon.* **5**, 770 (2011).
18. L. Gao, T. Zhu, M. Liu, and W. Huang, *Photon. Technol. Lett.* [Doi: 10.1109/LPT.2014.2361781](https://doi.org/10.1109/LPT.2014.2361781) (2014).
19. N. J. Smith, and N. J. Doran, *Opt. Lett.* **21**, 570 (1996).
20. X. Liu, X. Zhou, C. Lu, *Opt. Lett.* **30**, 2257 (2005).
21. Z. P. Sun, T. Hasan, F. Torrisi, D. Popa, G. Privitera, F. Q. Wang, F. Bonaccorso, D. M. Basko, and A. C. Ferrari, *ACS. NANO.* **4**, 803 (2010).
22. Q. L. Bao, H. Zhang, Y. Wang, Z. H. Ni, Y. L. Yan, Z. X. Shen, K. P. Loh, and D. Y. Tang, *Adv. Funct. Mater.* **19**, 3077 (2009).
23. E. Hendry, P. J. Hale, J. Moger, and A. K. Savchenko, *Phys. Rev. Lett.* **105**, 097401 (2010).
24. H. Zhang, S. Virally, Q. Bao, L. K. Ping, S. Massar, N. Godbout, and P. Kockaert, *Opt. Lett.* **37**, 1856 (2012).
25. Y. Lin, C. Yang, J. Liou, C. Yu, and G. Lin, *Opt. Express*, **21**, 16763 (2013).
26. Z. Luo, M. Zhou, D. Wu, C. Ye, J. Weng, J. Dong, H. Xu, Z. Cai, and L. Chen, *J. Light. Technol.* **29**, 2732 (2011).
27. B. Xu, A. Martinez, and S. Yamashita, *Photon. Technol. Lett.* **24**, 1792 (2012).
28. T. Gu, N. Petrone, J. F. Mcmillan, A. van der Zande, M. Yu, G. Q. Lo, D. L. Kwong, J. Hone, and C. W. Wong, *Nature Photon.* **6**, 554 (2012).
29. Y. Wu, B. Yao, Y. Cheng, Y. Rao, Y. Gong, X. Zhou, B. Wu, and K. S. Chiang, *Photon. Technol. Lett.* **26**, 249 (2014).
30. A. V. Gorbach, A. Marini, and D. V. Skryabin, *Opt. Lett.* **38**, 5244 (2013).
31. Z. Liu, X. H, and D. N. Wang, *Opt. Lett.* **36**, 3024 (2011).
32. L. Gao, T. Zhu, W. Huang, J. Zeng, *Appl. Opt.* **53**, 6452 (2014).

1. M. E. Fermann, and I. Hartl, "Ultrafast fibre lasers," *Nature Photon.* 7, 868-874 (2013).
2. X. Liu, D. Han, Z. Sun, C. Zeng, H. Lu, D. Mao, Y. Cui, F. Wang, "Versatile multi-wavelength ultrafast fiber laser mode-locked by carbon nanotubes," *Scientific reports* 3, 2718 (2013).
3. K. Kieu, W. H. Renninger, A. Chong, and F. W. Wise, "Sub-100 fs pulses at watt-level powers from a dissipative-soliton fiber laser," *Opt. Lett.* 34, 593-595 (2009).
4. M. Horowitz, Y. Barad, and Y. Silberberg, "Noiselike pulses with a broadband spectrum generated from an erbium-doped fiber laser," *Opt. Lett.* 22, 799-801 (1997).
5. L. M. Zhao, D. Y. Tang, J. Wu, X. Q. Fu, and S. C. Wen, "Noise-like pulse in a gain-guided soliton fiber laser," *Opt. Express* 15, 2145-2150 (2007).
6. L. M. Zhao, D. Y. Tang, T. H. Cheng, H. Y. Tam, and C. Lu, "120 nm bandwidth noise-like pulse generation in an erbium-doped fiber laser," *Opt. Commun.* 281, 157-161 (2008).
7. Y. Jeong, L. A. Vazquez-Zuniga, S. Lee, and Y. Kwon, "On the formation of noise-like pulses in fiber ring cavity configurations," *Opt. Fiber Technol.* 20, 575-592 (2014).
8. A. Runge, C. Aguergaray, N. Broderick, and M. Erkintalo, "Coherence and shot-to-shot spectral fluctuations in noise-like ultrafast fiber lasers," *Opt. Lett.* 38, 4327-4330 (2013).
9. T. North, and M. Rochette, "Raman-induced noiselike pulses in a highly nonlinear and dispersive all-fiber ring laser," *Opt. Lett.* 38, 890-892 (2013).
10. S. Lin, S. Hwang, and J. Liu, "Supercontinuum generation in highly nonlinear fibers using amplified noise-like optical pulses," *Opt. Express* 22, 4152-4160 (2014).
11. S. Keren, and M. Horowitz, "Interrogation of fiber gratings by use of low-coherence spectral interferometry of noiselike pulses," *Opt. Lett.* 26, 328-330 (2001).
12. D. Y. Tang, L. M. Zhao, and B. Zhao, "Soliton collapse and bunched noise-like pulse generation in a passively mode-locked fiber ring laser," *Opt. Express* 13, 2289-2294 (2005).
13. Q. Wang, T. Chen, M. Li, B. Zhang, Y. Lu, and K. P. Chen, "All-fiber ultrafast thulium-doped fiber ring laser with dissipative soliton and noise-like output in normal dispersion by single-wall carbon nanotubes," *Appl. Phys. Lett.* 103, 011103 (2013).
14. L. A. Vazquez-Zuniga, Y. Jeong, "Super-broadband noise-like pulse erbium doped fiber ring laser with a highly nonlinear fiber for Raman gain enhancement," *IEEE Photon. Technol. Lett.* 24, 1549-1551 (2012).
15. J. Schröder, T. D. Vo, and B. J. Eggleton, "Repetition-rate-selective, wavelength-tunable mode-locked laser at up to 640 GHz," *Opt. Lett.* 34, 3902-3904 (2009).
16. T. Herr, K. Hartinger, J. Riemensberger, C. Y. Wang, E. Gavartin, R. Holzwarth, "Universal formation dynamics and noise of Kerr-frequency combs in microresonators," *Nature Photon.* 6, 480-487 (2012).
17. F. Ferdous, H. Miao, D. E. Leaird, K. Srinivasan, J. Wang, L. Chen, L. T. Varghese, and A. M. Weiner, "Spectral line-by-line pulse shaping of on-chip microresonator frequency combs," *Nature Photon.* 5, 770-776 (2011).
18. L. Gao, T. Zhu, M. Liu, and W. Huang, "Cross-phase modulation instability in mode-locked laser based on reduced graphene oxide," *Photon. Technol. Lett.* Doi: 10.1109/LPT.2014.2361781 (2014).
19. N. J. Smith, and N. J. Doran, "Modulational instabilities in fibers with periodic dispersion management," *Opt. Lett.* 21, 570-572 (1996).
20. X. Liu, X. Zhou, C. Lu, "Four-wave mixing assisted stability enhancement: theory, experiment, and application," *Opt. Lett.* 30, 2257-2259 (2005).
21. Z. P. Sun, T. Hasan, F. Torrisi, D. Popa, G. Privitera, F. Q. Wang, F. Bonaccorso, D. M. Basko, and A. C. Ferrari, "Graphene Mode-locked ultrafast laser," *ACS. NANO.* 4, 803-810 (2010).
22. Q. L. Bao, H. Zhang, Y. Wang, Z. H. Ni, Y. L. Yan, Z. X. Shen, K. P. Loh, and D. Y. Tang, "Atomic-layer graphene as a saturable absorber for ultrafast pulsed lasers," *Adv. Funct. Mater.* 19, 3077-3083 (2009).
23. E. Hendry, P. J. Hale, J. Moger, and A. K. Savchenko, "Coherent Nonlinear Optical Response of Graphene," *Phys. Rev. Lett.* 105, 097401 (2010).
24. H. Zhang, S. Virally, Q. Bao, L. K. Ping, S. Massar, N. Godbout, and P. Kockaert, "Z-scan measurement of the nonlinear refractive index of graphene," *Opt. Lett.* 37, 1856-1858 (2012).
25. Y. Lin, C. Yang, J. Liou, C. Yu, and G. Lin, "Using graphene nano-particle embedded in photonic crystal fiber for evanescent wave mode locking of fiber laser," *Opt. Express*, 21, 16763-16776 (2013).
26. Z. Luo, M. Zhou, D. Wu, C. Ye, J. Weng, J. Dong, H. Xu, Z. Cai, and L. Chen, "Graphene-induced nonlinear four-wave-mixing and its application to multiwavelength Q-switched rare-earth-doped fiber lasers," *J. Light. Technol.* 29, 2732-2739 (2011).
27. B. Xu, A. Martinez, and S. Yamashita, "Mechanically exfoliated graphene for four-wave-mixing-based wavelength conversion," *Photon. Technol. Lett.* 24, 1792-1794 (2012).
28. T. Gu, N. Petrone, J. F. Mcmillan, A. van der Zande, M. Yu, G. Q. Lo, D. L. Kwong, J. Hone, and C. W. Wong, "Regenerative oscillation and four-wave mixing in graphene optoelectronics," *Nature Photon.* 6, 554-559 (2012).
29. Y. Wu, B. Yao, Y. Cheng, Y. Rao, Y. Gong, X. Zhou, B. Wu, and K. S. Chiang, "Four-wave mixing in a microfiber attached onto a graphene film," *Photon. Technol. Lett.* 26, 249-252 (2014).
30. A. V. Gorbach, A. Marini, and D. V. Skryabin, "Graphene-clad tapered fiber: effective nonlinearity and propagation losses," *Opt. Lett.* 38, 5244-5247 (2013).
31. Z. Liu, X. H, and D. N. Wang, "Passively mode-locked fiber laser based on a hollow-core photonic crystal fiber filled with few-layered graphene oxide solution," *Opt. Lett.* 36, 3024-3026 (2011).
32. L. Gao, T. Zhu, W. Huang, J. Zeng, "Vector rectangular-shape laser based on reduced graphene oxide interacting with long fiber taper," *Appl. Opt.* 53, 6452-6456 (2014).